Hindawi
Wireless Communications and Mobile Computing
Volume 2019, Article ID 9891821, 13 pages
https://doi.org/10.1155/2019/9891821

Research Article

Channel Coding for Multi-Carrier Wireless Partial Duplex

Hamid R. Barzegar and Luca Reggiani

Dipartimento di Elettronica, Informazione e Bioingegneria, Politecnico Di Milano, Milan, Italy

Correspondence should be addressed to Hamid R. Barzegar; hamidreza.barzegar@polimi.it

Received 13 September 2018; Revised 16 November 2018; Accepted 27 December 2018; Published 15 January 2019

Academic Editor: Simone Morosi

In order to leverage the spectrum resources, several forms of wireless duplex have been introduced and investigated in recent years. In Partial Duplex (PD) schemes, part of the band is transmitted in Full-Duplex (FD) and the rest in Half-Duplex (HD); therefore, some transmitted symbols will be characterized, at the receiver, by high SNR (Signal-to-Noise Ratio) and others by low SNR because of the residual self-interference (SI) in the FD part. Combining properly the patterns of these high and low SNR symbols affects the performance of the encoding schemes used in the system; in order to overcome this issue, different encoding and allocation schemes can be adopted for achieving a satisfactory solution. This paper investigates the performance of Low-Density Parity-Check (LDPC), turbo, polar codes for wireless PD. Orthogonal Frequency Division Multiplexing (OFDM) is an efficient multicarrier modulation technique, used in 4G and in the upcoming 5G, and it can be exploited for realizing a proper symbol allocation according to the SNR on each subcarrier. In this context, performance of LDPC, polar, and turbo codes derived from existing specifications has been studied when the system faces a mixture of high and low SNRs on the bits and hence on the symbols coming from the same codeword and this unbalanced SNR distribution is known a-priori at the transmitter, a condition associated with a scheme in which part of the symbols is subject to FD interference.

1. Introduction

Wireless mobile generations face a strong demand of services with high data rates to increasing numbers of connected users. In the next generation of cellular wireless mobile communication (5G) integrated technologies are expected to deliver high throughput with low latency and a really high number of connected devices. In order to achieve this objective, many design parameters related to complexity, latency, energy consumption, and bandwidth should be kept into account and addressed with innovative approaches.

Wireless systems, for either local or wide area networks, currently rely on Half-Duplex (HD) transmission with an orthogonal division of the two communication directions through separated time and/or spectral resources. Full-Duplex (FD) radio technology, which enables concurrent transmission and reception in the same spectrum at the same time, can boost the spectrum efficiency. However, FD communication has been implemented experimentally only for short-range transmissions and it is affected by numerous limitations even if, in the last two decades, many works have been reported in this area.

In order to increase the distance of FD communication, we proposed a Partial-Duplex (PD) approach [1], which consists of a communication link with the capability of supporting connection in both directions at the same time in a portion of the bandwidth (FD) and with a frequency division for uplink and downlink in the rest of the band (HD). Wireless Partial-Duplex (PD), according to its inherent nature, is meant to provide a way for relaxing the Self-Interference Cancellation (SIC) constraints at the receiver. Therefore, the objective is twofold: (i) increasing the transmission range and/or (ii) being able to operate with an SI canceler of lower performance and complexity since this is the most challenging component of an FD system. This PD scheme, characterized by the flexible mixing of HD and FD portions, is different from other schemes based on hybrid approaches: in [2–4], a partial overlap model named as *α-Duplex* is proposed, applicable to single-carrier

transmission, which relies on a proper selection of pulse-shaping and related matched filtering for optimizing the signals separation. In [5], the hybrid solution named *X-Duplex* consists of adapting links between full-duplex and half-duplex, for maximizing the system capacity: when the level of self interference is negligible, the link works on FD mode; otherwise, it switches to HD.

High spectral efficiency is one of the fundamental design targets in the wireless system and it is primarily affected by the selection of proper channel coding, modulation and this is clearly crucial also for FD and PD communication. In particular, it seems natural to start the investigation of encoding schemes for PD considering solutions based and adapted from the 4G and 5G standardization: 3GPP LDPC codes, which are excellent candidates for enabling also FD in the presence of residual self-interference, and the polar codes [6], introduced for control channels in 5G and 3GPP turbo codes.

What differentiates PD from HD and FD is the presence, in the same codeword, of a mixture of high and low SNR (Signal-to-Noise Ratio) conditions: in PD schemes, part of the band is transmitted in FD and the rest in half-duplex and, consequently, some transmitted symbols will be characterized by high SNR (i.e., symbols in the HD portion, denoted as high SNR symbols) and the others by lower SNR (i.e., symbols in the FD portion of the band, because of the residual self-interference of the system) according to a pattern which is known, a-priori, by the system. Combining properly the patterns of these high and low SNR symbols affects the coding performance of the system and this is one of the key design points for PD transmission. In this study, we show the performance achieved by different strategies for allocating low and high SNR symbols coming from the codewords derived and adapted mainly by the 4G and 5G 3GPP standards. We remark that one of the main peculiarities in this context is the a-priori knowledge of the positions in which high and low SNR symbols will be received since the transmission pattern between HD and FD parts is determined a-priori between transmitter and receiver. To the best of our knowledge, there are no studies that address specifically the problem of encoding codewords composed by bits with two different SNR levels at known positions in the codeword.

Performance of DVB-S2 (Digital Video Broadcasting-Satellite, 2^{nd} generation) LDPC codes with wireless partial duplex communication has been studied in [7]. This paper starts from the encoding solution presented in [7] and it extends it, providing the following main novel contributions:

(i) The comparison among different encoding solutions is extended to codes adapted from 5G LDPC [8], 4G turbo [9], and 5G polar codes [8]. In particular, it is found that the 5G LDPC solution presents some performance advantages for the PD transmission that are superior to the others, including the LDPC code studied in [7].

(ii) The encoding solutions are studied in the context of multi-carrier transmission, coherently with 4G and 5G waveforms.

(iii) The impact of channel frequency selectivity when it is included and integrated in the low and high SNR symbols allocation process is evaluated and discussed.

The rest of this paper is organized as follows. Section 2 revises briefly the channel coding schemes which they are studied and adapted here for PD. Then Section 3 presents the main concept and parameters of the PD scheme and the resulting system and channel models. The application of different encoding schemes to PD is presented in Section 4 and the allocation strategies in the multi-carrier waveform are presented in Section 5. Finally, the numerical results are reported and discussed in Section 6.

2. Coding Schemes

The 5G or New Radio (NR) will mark a transition also in Forward Error Correction (FEC) coding, according to Third Generation Partnership Project (3GPP) [8].

In [10], a comparison among convolutional, turbo, LDPC, and polar codes is presented, for different information block lengths and code rates. A study on candidates for channel coding in 5G in terms of Block-length-Error-Rate (BLER) and computational complexity for ultra-Reliable Low-Latency communication (URLLC) is provided in [11]. Different coding schemes for 5G short message transmission with a focus on error correction performance and complexity have been studied also in [12] and classes of rate-compatible LDPC code for URLLC with short message length and fast convergence have been studied in [13]. Finally, in [14], different coding schemes for 5G mobile broadband communication have been investigated. In the context of the design of LDPC codes for 5G communication, in [15], an approach is proposed and compared with turbo codes. A comprehensive comparison of channel coding schemes for 5G Machine Type Communication (MTC), one of the use-cases of 5G with short message transmission, has been presented in [12] and LDPC are compared to polar, turbo, and convolutional codes. The role of coding, high order modulation techniques in 5G, and satellite communication systems is considered in [16] and, in [17], successive interference cancellation schemes for a two-user non-orthogonal multiple access system using LDPC codes have been studied. In [18], the authors proposed a robust diversity-combining technique for the LDPC code to mitigate partial-band interference.

In terms of rate-compatibility for LDPC codes, the authors in [19] proposed a hybrid method based on the combination of parity puncturing and information shortening. The technique introduced in [20] and called shortening, generates codes of shorter length from a given LDPC code by putting an infinite reliability on some variable nodes; in this approach, the positions of these variable nodes are assumed to be available at the encoder and decoder sides.

In this paper, we have chosen to take and adapt to partial duplex communication the coding schemes and relative modifications available from 4G and 5G 3GPP standardization. This section presents briefly these encoding schemes, with a particular emphasis on LDPC codes.

2.1. LDPC Codes. LDPC codes [21] have attracted a great interest in the last 20 years, because of their effectiveness and decoder architecture. Nowadays, LDPC codes are applied to a variety of digital communication systems such as wireless local area networks, space communications, satellite digital video broadcasting and also the forthcoming cellular network (5G). LDPC codes are linear block codes characterized by a sparse parity check matrix, which allows iterative decoding based on message passing algorithms; one of the main decoding solutions, used here, is well-known as the sum-product algorithm [22]. They provide a performance that is very close to the capacity for many channels and decoding complexity which is linear with respect to codeword length. In addition, they admit implementations of the decoding process with large parallelism.

An LDPC code and its decoding process are typically represented through the Tanner graph, which reveals all the connections between the variable nodes (codeword bits) and the check nodes, i.e., the parity check equations in which they are involved (the rows in the parity check matrix). Each 1 in the parity check matrix is a connection between a check node (row) and a variable node (column). In order to have a good performance of the message passing algorithms, the presence of cycles in the Tanner graph, in particular of the minimum length 4, should be avoided.

Here, as a relevant example of high performance LDPC codes, we have considered the code designed for 5G with codeword length equal to 25344 bits [8]. Figure 1 illustrates the structure of the 5G LDPC parity check matrix. Denoting the input bit sequence as $b_0, b_1, b_2, b_3, \ldots, b_{B-1}$, if B is larger than the maximum code block size K_{cb}, a segmentation of the input bit sequence is done and an additional CRC sequence of $L = 24$ bits is attached to each code block. 5G LDPC is designed for rate 1/3 with a maximum code block size $K_{cb} = 8448, 3840$ and length $N = 25344$ and 11520, respectively. The total number of code blocks is determined by a specific algorithm [8]. The resulting parity-check matrix of 3GPP LDPC code H is composed of two parts, a dense part with a large number of non-zero elements in the left side and a sparse part with a small number of non-zero elements on each column and a diagonal shape in the right side, i.e.,

$$H = \left[H_{LDPC_1}, H_{LDPC_2}\right], \tag{1}$$

where H_{LDPC_1}, composed by 4 submatrices $\{H_1, H_2, H_4, H_5\}$, is the submatrix corresponding to the information bits and H_{LDPC_2}, composed by $\{H_3, H_6\}$, is a staircase lower triangular submatrix corresponding to parity bits (Figure 1). The staircase structure of H_{LDPC_2} is the basis for justifying one of the allocation strategies described in Section 5.

2.2. Turbo Codes. The Turbo Code (TC) concept, introduced in 1993 [23], is used in many applications such as 3G, 4G, and IEEE 802.16 (WiMAX). High decoding complexity, associated with long latency, is usually considered one of the main drawbacks of turbo decoding, due to the interleaving and the iterative process; in fact, one of the reasons for the selection of LDPC in 5G was the possibility of achieving higher computational efficiencies thanks to a parallelization

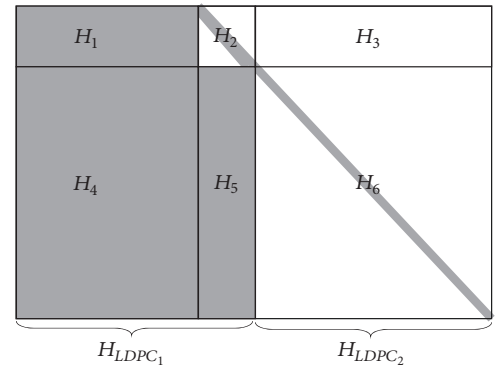

Figure 1: Structure of the 3GPP LDPC H matrix for 5G. The gray zones denote the areas in which the ones are distributed.

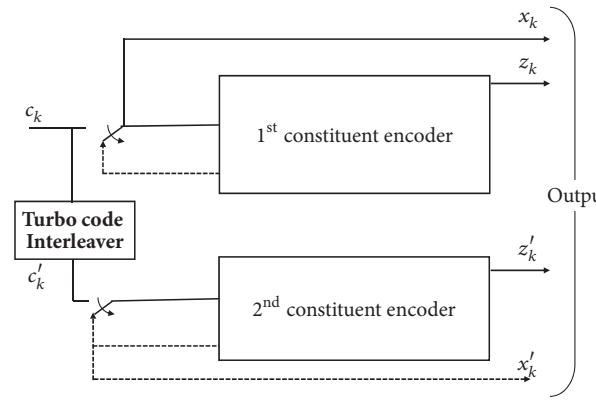

Figure 2: Structure of the rate 1/3 turbo encoder (dotted lines apply for trellis termination only) [9].

in the decoding process that is not possible for turbo decoding. In LTE, the turbo encoder [24] exploits a Parallel Concatenated Convolutional Code (PCCC) with two 8-state constituent encoders and one turbo code internal interleaver scheme. Figure 2 illustrates the structure of the LTE turbo code with code rate 1/3. The transfer function of the 8-state constituent code for the PCCC is

$$G(D) = \left[1, \frac{g_1(D)}{g_0(D)}\right] \tag{2}$$

where

$$\begin{aligned} g_0(D) &= 1 + D^2 + D^3, \\ g_0(D) &= 1 + D + D^3. \end{aligned} \tag{3}$$

The initial value of the shift registers of the 8-state constituent encoders shall be all zeros when starting to encode the input bits. The output from the turbo encoder is

$$\begin{aligned} d_k^{(0)} &= x_k \\ d_k^{(1)} &= z_k \\ d_k^{(2)} &= z'_k \end{aligned} \tag{4}$$

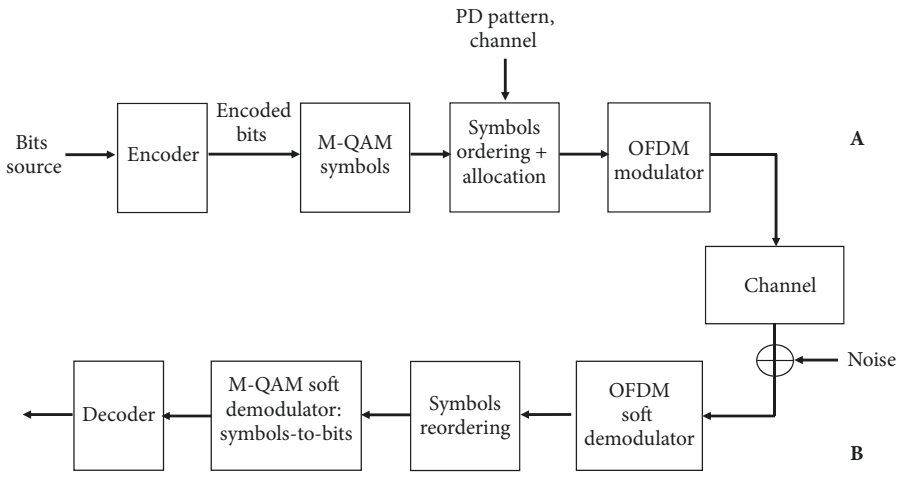

Figure 3: System model for partial duplex communication including the encoding and allocation blocks. Here B node is receiving from A.

for $k = 0, 1, 2, \ldots, K-1$. Turbo code input bits are denoted by $c_0, c_1, c_2, c_3, \ldots, c_{K-1}$, and the bits coming from the first and second 8-state constituent encoders are denoted by $z_0, z_1, z_2, z_3, \ldots, z_{K-1}$ and $z'_0, z'_1, z'_2, z'_3, \ldots, z'_{K-1}$, respectively. The bits from the turbo code internal interleaver are denoted by $c'_0, c'_1, \ldots, c'_{K-1}$, and these bits are the input of the second 8-state constituent encoder. LTE 3GPP turbo code uses trellis termination by taking the tail bits from the shift register feedback after all information bits are encoded. Tail bits are padded after the encoding of information bits. The first three tail bits are used to terminate the first constituent encoder (upper switch of Figure 2 in the down position) while the second constituent encoder is disabled. The last three tail bits shall be used to terminate the second constituent encoder (lower switch of Figure 2 in the down position) while the first constituent encoder is disabled.

2.3. Polar Codes. Polar codes are a recent class of channel coding introduced in 2009 with a novel concept called channel polarization [6]. The construction of a polar code is based on a recursive concatenation of a short code, transforming the physical channel into virtual channels whose reliability becomes very large or very small as the number of recursions increases (channel polarization). Associating the data bits with the most reliable virtual channels allows achieving the capacity for the symmetric binary-input, discrete, memoryless channels. From a mathematical point of view, polar codes are generated by the Kronecker recursive product of the following kernel code:

$$G_2 = \begin{bmatrix} 1 & 0 \\ 1 & 1 \end{bmatrix}. \tag{5}$$

Therefore, the encoder of an (N, K) polar code with a length of $N = 2^n$ is the following n^{th} Kronecker power:

$$G_N = \left(G_2\right)^{\otimes n}, \tag{6}$$

and the polarization effect creates N virtual channels, each one experiencing a different reliability; message bits are allocated to the K most reliable channels and the others are *frozen* to fixed values, typically zeros, known at receiver and transmitter. The codeword c is obtained by

$$c = u \cdot G_N, \tag{7}$$

where u is the input vector $\{u_0, u_1, \ldots, u_{N-1}\}$, generated by assigning value 0 to all the frozen bits and the information message bits to the remaining positions.

A comparison among several well-known polar code constructions with the aim of finding the best design-SNR polar code construction has been studied in [25]. On the other hand, in terms of length-compatibility, a design for wide range of lengths in polar codes has been studied in [26]. Polar codes have attracted great interest also in the 5G standardization, thanks to the excellent performance in binary input discrete memoryless channels under low complexity successive cancellation (SC) decoding. The 5G polar sequence encoding is given in [8] and a description of the encoding process can be found in [27].

3. System Model for Partial Duplexing

Let us consider a bidirectional link between two nodes, A and B, and assume that the link characteristics are reciprocal, from A to B and B to A. Two OFDM signals, one for each direction, occupy a total bandwidth equal to B [Hz] in N_{SC} subcarriers. The modulations for each subcarrier are QAM with 16 or 256 levels since we are interested to the highest spectral efficiencies. Figure 3 presents the chain of the fundamental blocks of our system: the bits are encoded (LDPC, turbo or polar), modulated through the selected M-QAM modulation and the resulting symbols are allocated to the OFDM subcarriers according to a specific allocation scheme, which depends primarily on the partial duplex pattern and, possibly, also on the channel. At the receiver, the soft demodulators provide the input likelihood information about the bits to the final decoders (LDPC, turbo or polar).

The wireless propagation channel model between A and B, assumed reciprocal in the two directions, is modeled by

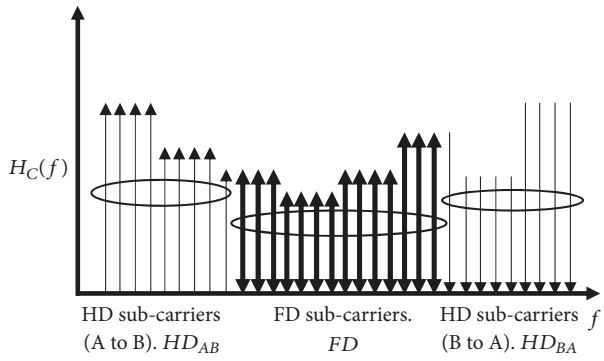

Figure 4: Block strategy for OFDM partial duplex.

a flat frequency path loss contribution (PL) and a random fading frequency selective transfer function $H_C(f)$. The study has been conducted for two channel models:

(i) Ideal channel model that introduces only additive white Gaussian noise with power spectral density N_0 (AWGN), assuming all over the bandwidth a normalized channel transfer function $H_C(f) = 1$.

(ii) Frequency selective fading channel model where the received signal on the $i-th$ subcarrier at frequency f_i is affected by the channel transfer function $H_C(f_i) = H_i$. The frequency selective channel is simulated by a Rayleigh channel model with different coherence bandwidths. In case of Rayleigh fading model, in order to reproduce the general impact of a frequency selective channel according to the coherence bandwidth definition B_C (the range of frequencies over which the channel response is highly correlated), the bandwidth of the signal is divided into equal subbands of width B_C [Hz], where the channel is assumed flat. As the representative of the channel frequency selectivity, the single parameter $\lambda_C = B_C/B$ allows reproducing the frequency selectivity effect of different channel models.

The PD solution for multi-carrier transmission has been introduced in [1] with the aim of extending the range of FD communication; in its simplest form, PD can be applied to a block of adjacent carriers or subchannels (Figure 4). The Partial Duplex Parameter (PDP) is the fundamental factor of PD, which returns the overlapped portion of the spectrum between uplink and downlink. The number of subcarriers interested by overlapped bandwidth and full duplex is simply

$$N_{FD} = PDP \cdot N_{SC}, \tag{8}$$

and those interested by transmission on one direction, uplink and downlink, (or HD) are

$$N_{HD} = 0.5 \cdot (1 - PDP) \cdot N_{SC}. \tag{9}$$

Therefore, the total number (HD and FD) of uplink and downlink subcarriers is equal to

$$N_{FD} + N_{HD} = 0.5 \cdot (1 + PDP) \cdot N_{SC}, \tag{10}$$

Table 1: Main parameters of the system.

Parameters	Turbo	Polar	5G LDPC	DVB-S2
Code Lengths		*N = 528, 2112*		*540,2160*
Code rate		*1/3*		
Channel		*AWGN*		
Modulation		*BPSK, 16 QAM, 256 QAM*		
Δ		*30 (dB)*		
High SNR (HD)		*-10:30 (dB)*		
Low SNR (FD)		*SNR_High – Δ (dB)*		
PDP		*(Partial Duplex Parameter)*		*[0.1:0.1:1]*
B		*40 MHz*		
N_{SC}		*66, 264*		*68, 270*
CRC	*N/A*	*8*	*N/A*	
Decoder	*a-posteriori probability*	*SCL, L=8*	*Sum-Product*	

generating an overall potential throughput gain with respect to HD transmission proportional to $(1 + PDP)$ but, of course, affected by a different SNR level (possibly with a very high SNR gap) in the FD portion. The difference between the SNR found at HD and FD subcarriers, a crucial parameter in the code design, is denoted as Δ [dB] and it is assumed fixed in all the bandwidth. In other words, Δ models the impact on the SNR of the portion of self-interference that is not completely cancelled by the SIC; its fixed value, constant throughout the bandwidth, is a simplified assumption since a real SIC has generally a frequency response that is not ideal. However, in this study, Δ should be interpreted as an average value and the SIC frequency variations included in the frequency selective fading channel model, where each subcarrier response $H_C(f_i)$ can be differentiated according to different coherence bandwidths, until the single subcarrier level, as it will be shown in the numerical results.

Finally, we remark that the significant difference between the PD scheme and other schemes is in the flexibility of the bandwidth overlapping, without constraints on pulse filtering; being the system based on multi-carrier transmission, the channel frequency selectivity can be exploited for allocating the symbols and the FD subcarriers according also to the SNR conditions (Figure 5); this selective and block strategies have been proposed in [1] and Section 5 will provide more details about the exploitation of this opportunity integrated with the encoding and allocation process. The main parameters of the simulated system are listed in Table 1.

4. Encoded Wireless Partial Duplex

Partial-duplex is an intermediate solution between HD and FD which was proposed in order to (i) increase the overall bidirectional system data rate with respect to classical HD and (ii) limit performance degradation in FD. In fact, FD transmission may suffer from the heavy impact of residual self-interference, not completely compensated by SI cancelers. In the next subsections, we present the PD system and the codes adopted in this study. In order to evaluate the performance of

Table 2: Encoding solutions for the PD schemes.

Encoding	S	N	K	R	N_{SC}
DVB-S2	*64800/120*	*540*	*180*	*1/3*	*68*
	64800/30	*2160*	*720*		*270*
5G	*25344/48*	*528*	*172*	*1/3*	*66*
	25344/12	*2112*	*704*		*264*
Turbo	*N/A*	*528*	*172*	*1/3*	*66*
		2112	*704*		*264*
Polar	*N/A*	*528*	*172*	*1/3*	*66*
		2112	*704*		*264*

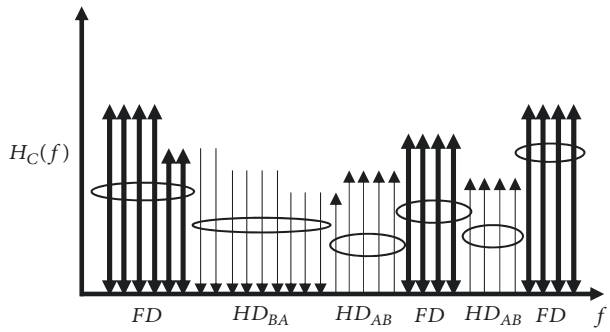

Figure 5: Selective strategy for OFDM partial duplex.

the proposed system, we have adapted the design of the codes resumed in Section 2:

(i) 5G LDPC with rate $R = 1/3$ and codeword lengths equal to $N = 528$ and $N = 2112$.

(ii) DVB-S2 LDPC, for assuring a comparison with our previous work [7], which was based on the LDPC design for DVB-S2. Again $R = 1/3$ and the codeword lengths are $N = 540$ and $N = 2160$. The length of the DVB-S2 codeword and node indexes parameter are $N = 64800$ and $N_B = 360$ in the original structure.

(iii) 5G Polar Code with rate $R = 1/3$ and codeword lengths equal to $N = 528$ and $N = 2112$.

(iv) 4G Turbo Code with rate $R = 1/3$ and codeword lengths equal to $N = 528$ and $N = 2112$.

The encoding solutions are summarized in Table 2; the scaling factor S, explained in Section 4.1, is used to reduce the length of the LDPC codes from the original maximum codeword. The next sections are explaining the main modifications and assumptions made with respect to the original codes resumed in Section 2.

4.1. LDPC Codes for PD. For LDPC codes, the parity check matrix is designed for a specific input block length, which is different from those needed in Partial Duplex schemes, according to the variability of the overlapping portion of the subcarriers. In order to change the codeword length, the original 3GPP 5G and DVB-S2 codes are scaled preserving their structure and rate, as done in [7] for the DVB-S2 LDPC with $R = 1/2$.

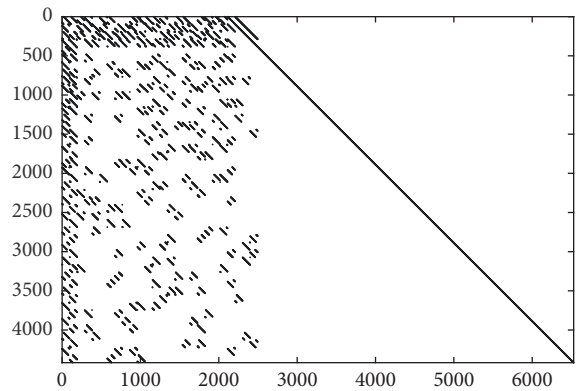

Figure 6: Final structure of the LDPC H matrix with codeword length equal to 6336 and rate 1/3 derived from 3GPP [8].

The scaling process extracts the upper-left submatrices of the matrices H_1, H_2, H_4, H_5 in Figure 1, leaving H_3 empty and H_6 with the same diagonal structure. Starting from the original 5G codeword length and information bits $N' = 25344$ and $K' = 8448$, in order to preserve the original structure and rate, we apply a scaling integer factor S to the original matrix. For obtaining a new codeword with K information bits, we consider a scaling factor S that respects the conditions

$$mod\left(K', S\right) = 0 \tag{11}$$

and

$$mod\left(N', S\right) = 0, \tag{12}$$

obtaining a new codeword length

$$N = \frac{N'}{S} \tag{13}$$

and a new node indexes parameter

$$N_B = \frac{N'_B}{S}. \tag{14}$$

Table 3 reports all the codes that can be obtained from this simple scaling procedure. Here the DVB-S2 and 3GPP 5G H matrices are scaled initially to the size 4320×6480 and 4416×6528, with code rate 1/3, respectively (namely, in the 5G LDPC we have considered $M_{cb} = 8448$ but the same is applicable also to $M_{cb} = 3840$). Figure 6 shows the H matrix structure of 3GPP 5G structure after scaling with scale factor $S = 4$ and Figure 7 the H matrix derived from DVB-S2 with $S = 10$. After this step, the matrices are further scaled of factors 12 and 3 for obtaining the final lengths around 500 and 2100. Figure 8 shows the comparison of the weights distribution per column in the 5G and the DVB-S2 LDPC H matrices for rate 1/3 after scaling. At the decoder side, a sum-product algorithm with 50 iterations is applied.

4.2. Turbo Codes for PD. Here the turbo code with lengths $N = 528$ and $N = 2112$ is obtained by exploiting a trellis

Table 3: List of original [$S = 1$] and modified codes with scaled S, K, and N.

S	1	2	3	4	6	8	12	16	24	32	48	64	96	128	192	384
K	8448	4224	2816	2112	1408	1056	704	528	352	264	176	132	88	66	44	22
N	25344	12672	8448	6336	4224	3168	2112	1584	1056	792	528	396	264	198	132	66

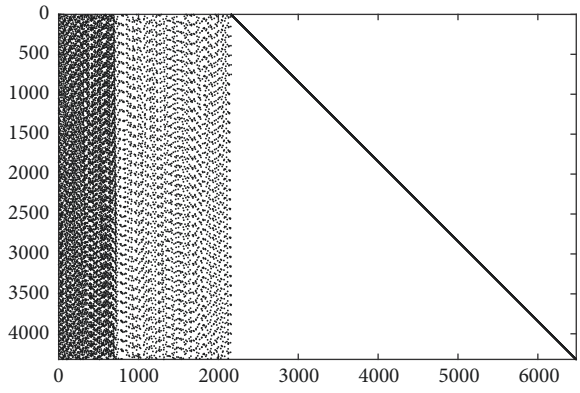

Figure 7: Final structure of the LDPC H matrix for codeword length equal to 6480 bits and rate 1/3 derived from DVB-S2.

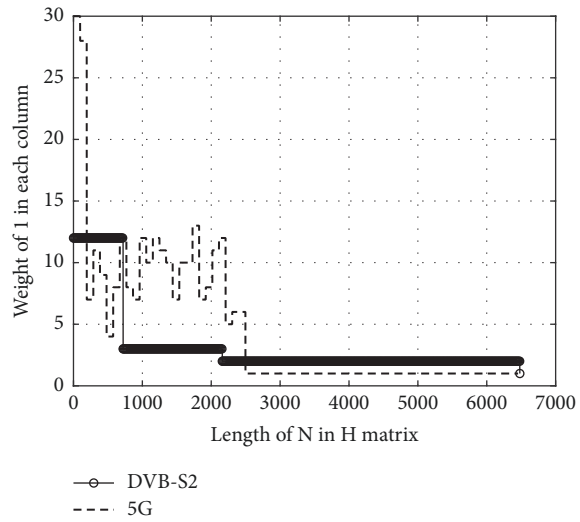

Figure 8: Comparison of the weights per column in the 5G and the DVB-S2 LDPC H matrices for rate 1/3 after first scaling.

termination of the codes involved in the scheme described in Section 2.2. At the decoder side, a max-log-MAP algorithm with 8 iterations is applied.

4.3. Polar Codes for PD. Here the polar code with lengths $N = 528$ and $N = 2112$ is obtained by exploiting the algorithm and the interleaving pattern in [8]. At the decoder side, the Successive Cancellation List (SCL) algorithm is applied.

5. Allocation of Encoded Bits

In the system, after encoding the bits through the encoder and modulating them into 16-QAM, 256-QAM or BPSK symbols, as sketched in Figure 3, the vector of symbols will be allocated according to specific patterns based on the low or high SNR due to the presence of subcarriers operating in full or half duplex. In addition to the reference, random-based strategy, we are validating also a different allocation denoted as a positioning strategy, introduced in [7] and adapted here to the multi-carrier transmission. This strategy follows from the specific structure of the LDPC parity check matrix: the symbols coming from the left part of the codeword are allocated in the subcarriers that will be characterized by high SNR and all the symbols coming from the right part of the codeword in the subcarriers with lower SNR (FD), obviously according to the *PDP* of the system. In practice, the symbols are allocated starting from the left to the right of the codeword to the subcarriers from the highest to the lowest predicted SNRs. The rationale behind this strategy is that in the right part of the LDPC matrix (corresponding to H_{LDPC_2} in the original structure (1)), the bits are involved in a low number of parity check equations and, consequently, the impact on the overall performance of low SNR conditions could be more limited here. As an example, if we consider $PDP = 0.5$, HD bits (and corresponding symbols) with high SNR, from 0 to 264, are located in the left side of H (corresponding to H_{LDPC_1} in (1)) and bits with low SNR are located in the right side from position 265 to 528 with scaling equal to $S = 48$. In [7] we remarked that this allocation relies on the DVB-S2 code structure and the 3GPP 5G LDPC also follows a similar structure for the H matrix; however, this approach is not giving advantage for general LDPC codes and, as it will be verified in the numerical results, in other codes that do not share the same structure of the parity check matrix. After passing through the channel, the signal at the receiver side is processed and reordered according to the allocation procedure.

When we consider, in the multi-carrier transmission, the exploitation of frequency selectivity we proceed by making a preliminary allocation of the subcarriers to FD or HD transmission according to the channel gain in each subcarrier (or, more generally, group of sub-carriers). Therefore, the allocation of subcarriers to FD transmission is based on the channel, since subcarriers with highest SNRs are allocated to FD transmission and the others to HD according to the system PDP value. This step is referred here as frequency selective allocation and, after this step, each sub-carrier k will be characterized by an expected SNR level SNR_k, due to the channel power gain $|H_k|^2$ and to the FD or HD transmission. In the case of FD transmission, the expected SNR is estimated by considering, with respect to a reference level SNR_0, the impact of channel and self-interference as

$$SNR_k\,(FD) = SNR_0 + 10 \cdot \log_{10} |H_k|^2 - \Delta, \tag{15}$$

while, in the HD case, only the channel gain is considered, i.e.

$$SNR_k\,(HD) = SNR_0 + 10 \cdot \log_{10} |H_k|^2 . \tag{16}$$

We remark that, in the case of selective strategy, transmitter and receiver will need to know and update periodically the channel gains at the different subcarriers (or the resulting SNRs) as in any adaptive allocation technique; this challenging aspect is generally addressed by inserting appropriate pilots patterns in the OFDM frame and using a feedback control channel reporting the channel status at the transmitters sides. Finally, let us summarize the allocation strategies of the vectors of symbols in the subcarriers:

(i) Positioning strategy: in this strategy, following from the specific structure of the DVB-S2 and 3GPP 5G parity check matrix, the symbols are allocated starting from the left of the codeword to the subcarriers with HD transmission. After finishing the HD subcarriers according to the particular *PDP* value, the rest of the symbols will be allocated to the FD subcarriers until the end of the codeword. In the case of turbo and polar codes, we have verified that the structure of the parity check matrix does not allow a simple separation of the symbols between low and high weight symbols as in the LDPC cases considered here. Therefore, the positioning strategy is applied to polar and turbo codes just leaving the systematic part, where available, on the right part of the codeword, allocated starting from the FD subcarriers.

(ii) Random strategy: here, positions of the symbols are distributed randomly among the subcarriers, regardless of their expected SNR. Random distribution serves as a reference performance curve.

(iii) Positioning strategy with frequency selective allocation: the expected SNRs used for the positioning strategies are determined taking into account the channel gains. The FD subcarriers are preselected starting from the most favorable channel gains.

(iv) Random strategy with frequency selective allocation: the allocation of the symbols is random but the FD subcarriers are preselected starting from the most favorable channel gains.

6. Numerical Results

The different strategies described in Section 5 are compared here with different modulations, encoding, and system parameters. The SNR is computed as the ratio between the mean energy per information symbol E_S and the AWGN one-sided power spectral density N_0. Figure 9 presents a comparison among the error rates obtained from the different types of encoding schemes used in this study in AWGN. The best achieved performance is achieved by the turbo code with $N = 2112$, about 1 dB with respect to LDPC with $N = 528$ at $BER = 10^{-7}$. This performance comparison refers to a standard HD transmission, so without use of partial or full duplex. Numerical results regarding PD tradeoffs are organized into two sections: the first (Section 6.1) is focused on the pure performance of the codes, enforced by the subcarriers allocation in presence of high and low SNR due to the partial or full duplex, and the second (Section 6.2)

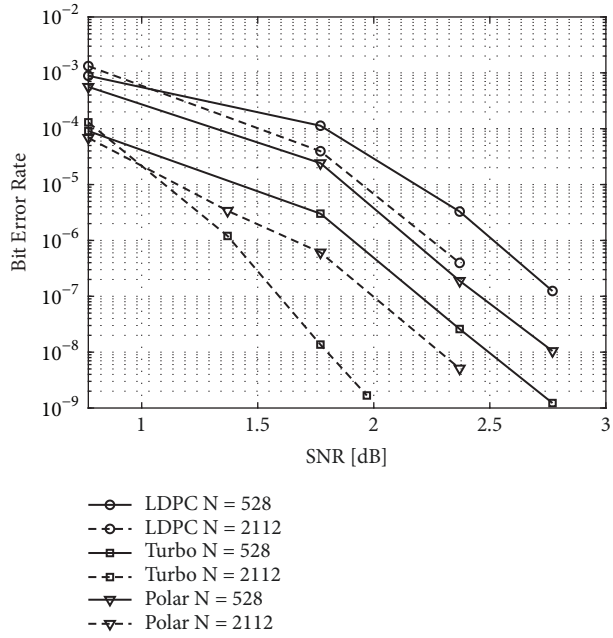

Figure 9: Comparison of 5G LDPC, turbo, and polar codes performance, rate 1/3, BPSK modulation and ideal channel (AWGN). Solid lines are for $N = 528$ and dashed lines for $N = 2112$.

introduces also the impact of channel selectivity on the overall performance. The difference between low and high SNR due to the full duplex transmission is $\Delta = 30$ dB unless stated otherwise.

6.1. Ideal Channel. An ideal channel propagation, characterized only by AWGN, allows showing the pure contribution of the code associated to the different levels of partial duplexing (expressed by the parameter PDP). Figure 10 presents the *SNR* vs *PDP* for obtaining a target $BER = 10^{-5}$ with a rate equal to 1/3 and codeword lengths $N = 528$ for 5G LDPC and 16-QAM modulation; Figure 10 shows that the best results are obtained always for the positioning strategy, for either the 16-QAM and 256-QAM modulation. We can notice that all the curves converge to the same performance values for $PDP = 0$ and $PDP = 1$, corresponding to HD and FD systems, respectively; in these two cases, all the subcarriers are characterized by the same SNR (high in the HD case and low in the FD one) and, in addition, performance gap turns out to be clearly equal to parameter Δ (Table 1). Figure 11 presents the same type of results for the longer codeword, $N = 2112$. This setup shows a similar behavior of the system and the positioning strategy has always the best performance with respect to others, with a maximum difference around 8 dB at $PDP = 0.5$.

Figure 12 shows a direct comparison between the positioning strategy and a random allocation (symbol or bit level) for the polar code with similar length. It is interesting to notice that the polar code shows always a similar behavior, independently from the strategy applied to the system and this is due to the different structure of the parity check matrix,

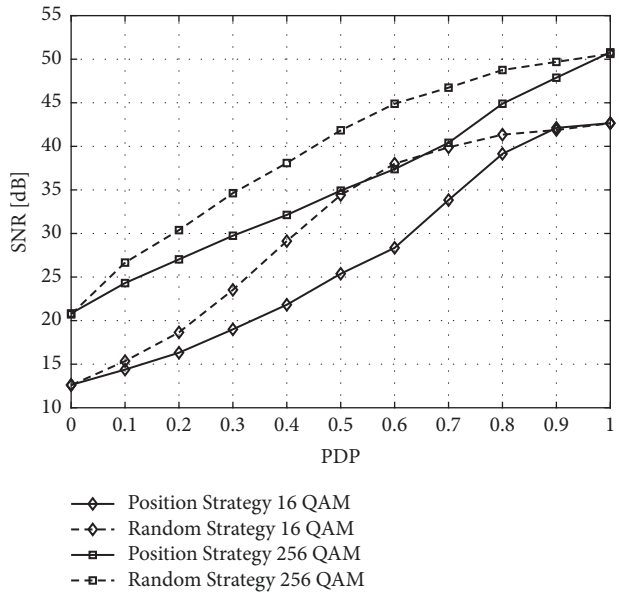

FIGURE 10: *SNR* necessary for achieving a $BER = 10^{-5}$ versus *PDP* in ideal channel (AWGN). Codeword length $N = 528$, rate $R = 1/3$ for 5G LDPC. Dashed lines refer to random strategy and solid ones to positioning strategy. Diamond markers refer to 16-QAM and square ones to 256-QAM.

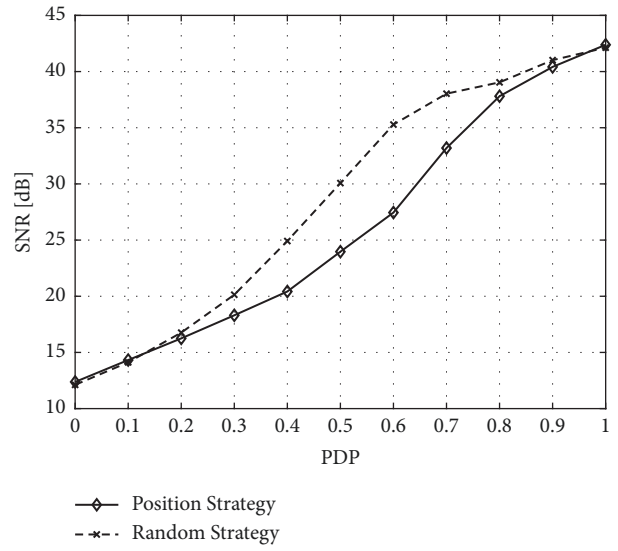

FIGURE 11: *SNR* necessary for achieving a $BER = 10^{-5}$ versus *PDP* in ideal channel (AWGN). Codeword length $N = 2112$, rate $R = 1/3$ for 5G LDPC and 16-QAM modulation. Dashed lines are for random strategy and solid lines for positioning strategy.

which is important for the application of the positioning strategy.

Similarly, Figure 13 compares different strategies for the 4G turbo code. In this case, the positioning strategy has the worst performance, as concentrating in any way the low SNR bits in adjacent positions of the codeword damages the convergence and quality of the turbo decoding, which takes inherently advantage of the randomness of the information

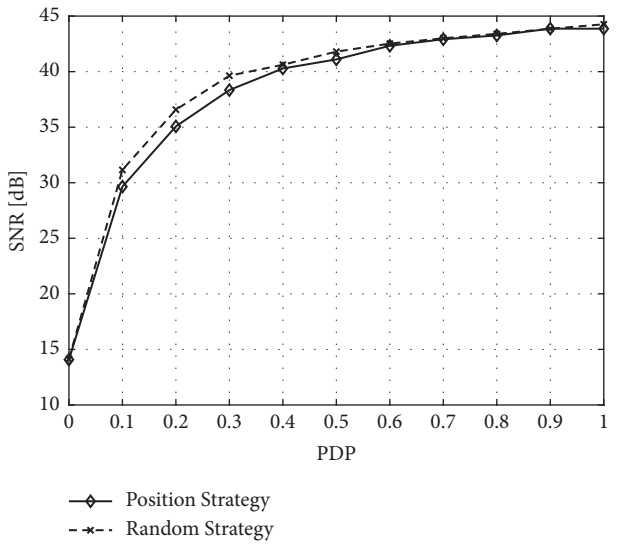

FIGURE 12: *SNR* necessary for achieving a $BER = 10^{-5}$ versus *PDP* in ideal channel (AWGN). Codeword length $N = 528$, $R = 1/3$ for 5G polar code and 16-QAM modulation. Dashed lines are for random strategy and solid lines for positioning strategy.

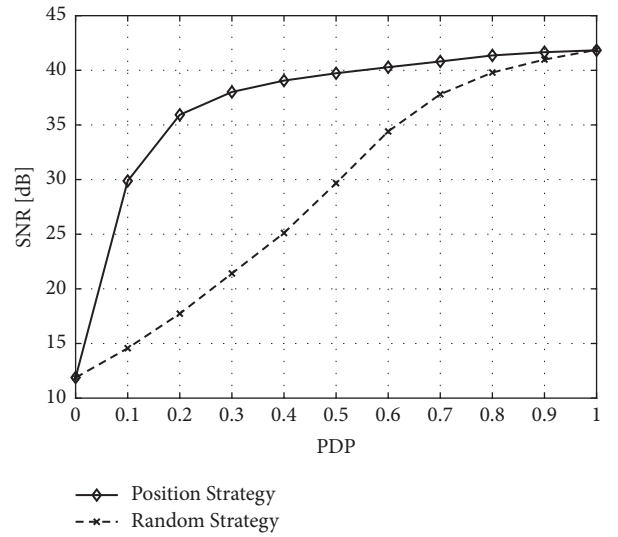

FIGURE 13: *SNR* necessary for achieving a fixed $BER = 10^{-5}$ versus PDP, rate 1/3 with $N = 528$ for 4G turbo, under AWGN channel and 16-QAM modulation. Dashed lines are for random strategy and solid lines for positioning strategy.

contributions from each symbol. It is clear that the simple random strategy is the right choice and turbo codes are a correct choice with respect to other coding schemes for Partial-Duplex if we do not want to use the apriori information about the expected SNR at the subcarriers.

From all the numerical results, it appears clearly that the selected LDPC codes, for the structure of their parity check matrices, offer the best performance for the subcarrier allocation based on the positioning strategy. A further comparison between the two LDPC codes adapted here (5G and DVB-S2) reveals the best design choice for the PD system:

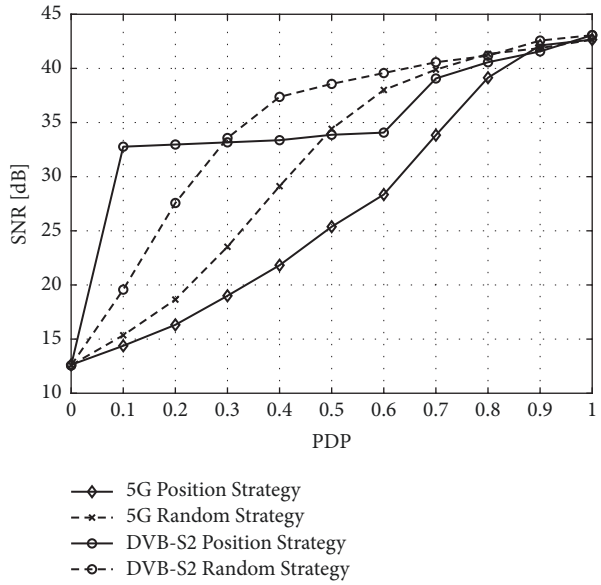

Figure 14: *SNR* necessary for achieving a fixed $BER = 10^{-5}$ versus *PDP*. $N = 528$ for 5G LDPC and $N = 540$ for DVB-S2 LDPC, in ideal channel (AWGN) and 16-QAM modulation. Dashed lines are for random distribution and solid lines for positioning strategy.

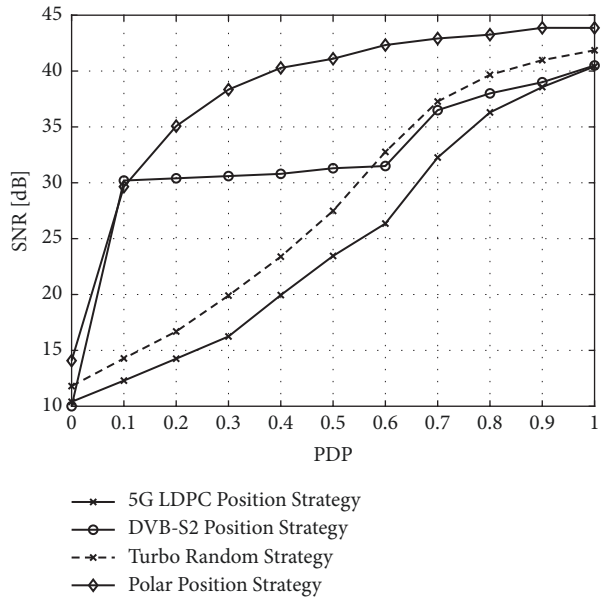

Figure 15: *SNR* necessary for achieving a fixed $BER = 10^{-5}$ versus *PDP*. $N = 528$ for 5G LDPC, turbo code, polar code and $N = 540$ for DVB-S2 LDPC, in ideal channel (AWGN) and 16-QAM modulation.

Figure 14 presents the *SNR* vs *PDP* at a fixed $BER = 10^{-5}$ with codeword lengths $N = 528$ and $N = 540$ for 5G and DVB-S2 LDPC codes in an ideal channel and 16-QAM modulation: the random bit strategies for both cases are a good choice for low PDP, i.e., $PDP < 0.4$ but, for $PDP > 0.4$, the behavior of the system changes and the positioning strategy turns out to be the best choice until $PDP = 0.6$. For $PDP > 0.6$, all the strategies achieve approximately the same performance, as the impact of the large portion of low SNR symbols at the corresponding subcarriers nullifies any allocation strategy of the few high SNR symbols in the codeword. Nevertheless, the performance of the 5G LPDC with positioning strategy is always the best, showing an advantage around 3 dB at $PDP = 0.5$ with respect to 5G LDPC with random strategy and DVB-S2 with positioning and about 12 dB with respect to DVB-S2 with random strategy.

In order to focus on an exhaustive comparison, Figure 15 reports the best results of the different schemes. It is clear that the performance of 5G LDPC code is better than the DVB-S2 LDPC, which has a similar shape of H matrix but different weights distribution of non-zero elements in the $H1$ part. In particular, the difference between 5G and DVB-S2 LDPC codes at medium-low values of PDP for the position strategy can be explained by the different distribution of ones in the parity check matrices, shown in Figures 6–8. 5G LDPC code has a higher number of ones in the left part of the matrix, allocated to the high SNR bits; this higher number of relations among the encoded bits helps to recover the correct decoding when part of the bits on the right side become affected by high interference. The DVB-S2 matrix is less robust from this point of view, as the presence of low SNR bits in the right part immediately degrades performance (from $PDP = 0.1$). Therefore, the best condition for applying the position strategy turns out to be a parity check matrix with a part containing a low number of ones (where to concentrate the low SNR bits) and another part with a reasonably high number of ones (compatible with the cycles constraints in LDPC codes) where to concentrate the high SNR bits.

At the same time, the turbo code with random strategy is the best encoding and allocation choice when we do not use the a-priori knowledge of the positions of the sub-carriers with high and low SNR, especially for $PDP < 0.6$. Figure 16 presents the same results but for codeword length $N = 2112$. This setup is characterized by a similar behaviour of the system.

Finally let us evaluate the impact of Δ: Figure 17 compares different values $\Delta = \{20, 30, 45, 50\}$ [dB] for a fixed $BER = 10^{-5}$ and rate $R = 1/3$, $N = 528$ in 16-QAM modulation for 5G LDPC coding; results appear shifted but they do not change significantly from a qualitative point of view. Similar conclusions are obtained with $N = 2112$. Figure 18 compares different values of the parameter $\Delta = \{20, 30, 45, 50\}$ [dB] for the 4G turbo code in the same conditions and the results do not show relevant differences as well.

6.2. Selective Channel with Fading. The study in case of channel affected by multipath with the relative frequency selectivity has been focused on the 5G LDPC code according to the result obtained in Section 6.1. The channel selectivity, as explained in Section 3, is exploited by including the low and high SNR evaluation for each subcarrier, the effect of the channel response; this increases the expected performance at the expense of the system implementation, which becomes more complicated since it has to respect the following assumptions and operations:

(i) The channel knowledge is needed at the transmitter, as in any adaptive allocation strategy based on channel response selectivity.

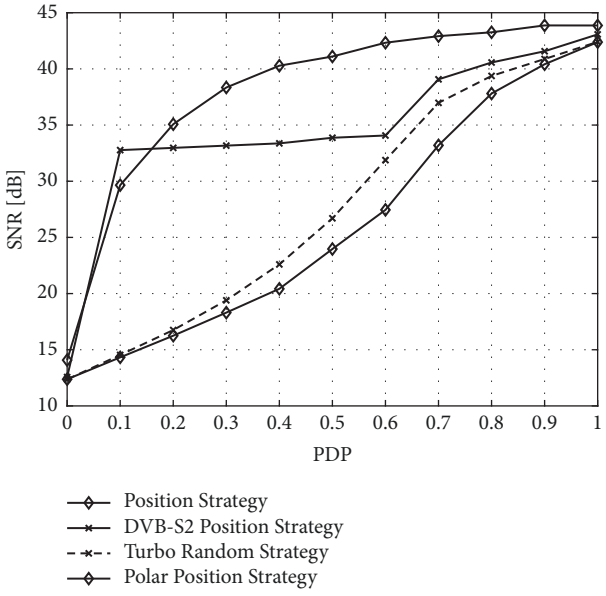

Figure 16: *SNR* necessary for achieving a fixed $BER = 10^{-5}$ versus P*DP*. $N = 2112$ for 5G LDPC, turbo code, polar code and $N = 2160$ for DVB-S2 LDPC, under AWGN channel and 16-QAM modulation.

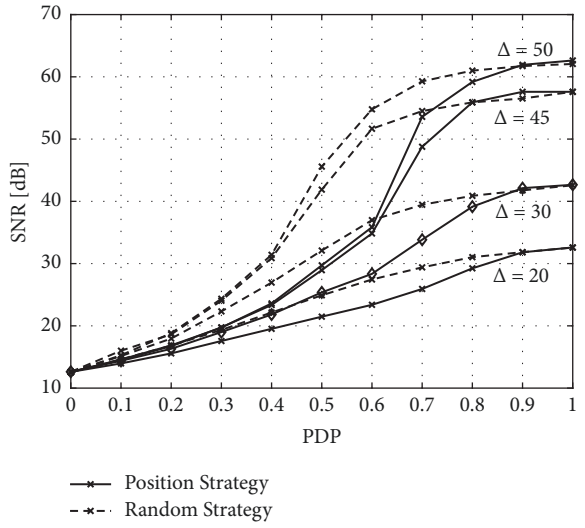

Figure 17: Comparison among different values of Δ for $N = 528$ and 5G LDPC code at $BER = 10^{-5}$ with 16-QAM modulation.

(ii) The allocation of subcarriers to FD transmission is based on the channel, since subcarriers with highest SNRs are allocated to FD transmission and the other to HD according to each PDP value.

(iii) The final allocation of the encoded symbols, following the strategies in Section 5 (in particular, the positioning one), is performed according to the SNRs values at each subcarrier.

Figure 19 compares different strategies with and without frequency selective allocation for $PDP = 2/3$ and $\lambda = 0.25$. It is clear the great advantage given by selecting the

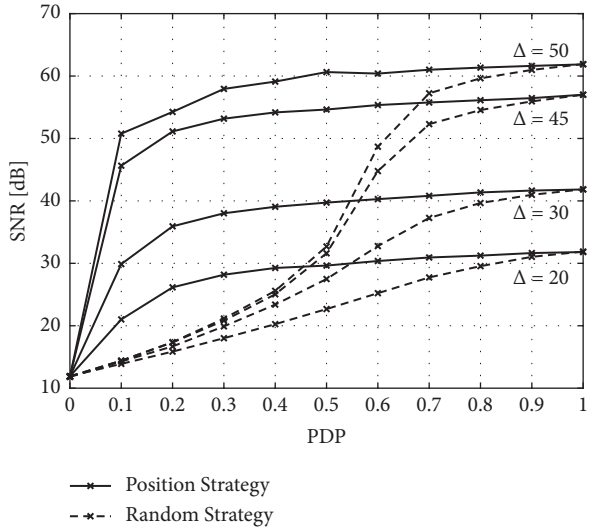

Figure 18: Comparison among different values of Δ for $N = 528$ and 4G turbo code at $BER = 10^{-5}$ with 16-QAM modulation.

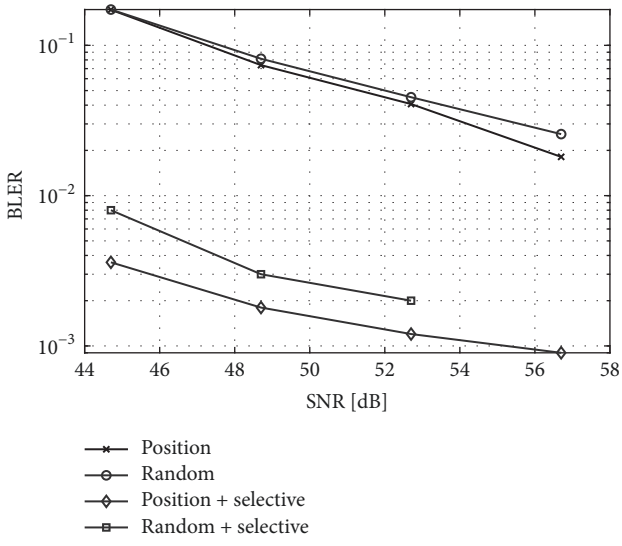

Figure 19: Comparison among different strategies with and without frequency selective allocation. Modulation is 256-QAM, $PDP = 0.6667$, $\lambda = 0.25$ and $N = 2112$.

positions of the low SNR symbols, in both positioning and random strategies, including channel and consequently SNR conditions; also in this case, the performance of the positioning strategy is better than the random one.

Figure 20 shows the different strategies for $PDP = \{0, 0.5, 1\}$ and Figure 21 for $PDP = 0.5$ but different values of λ ($\lambda = \{0.25, 0.5, 1.0\}$). According to the results, the positioning strategy applied to 5G LDPC, combined with the frequency selective allocation, assures the best performance.

7. Conclusions

In this paper, we have studied encoding and allocation techniques for improving performance of partial-duplex systems

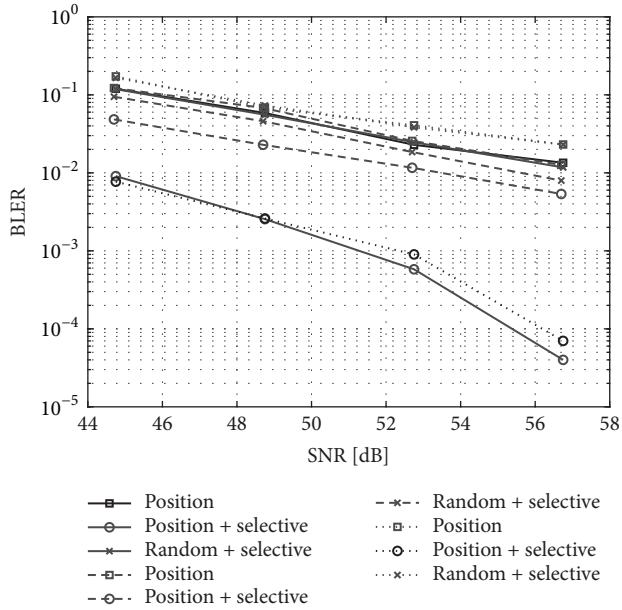

Figure 20: *BLER* versus *SNR* for different *PDP* and different strategies, rate 1/3 for 5G LDPC, with $\lambda = 0.25$, 256-QAM modulation and $N = 1056$. Curves with solid lines are for *PDP* = 0, curves with dashed lines are for *PDP* = 0.5 and curves with dotted lines for *PDP* = 1.

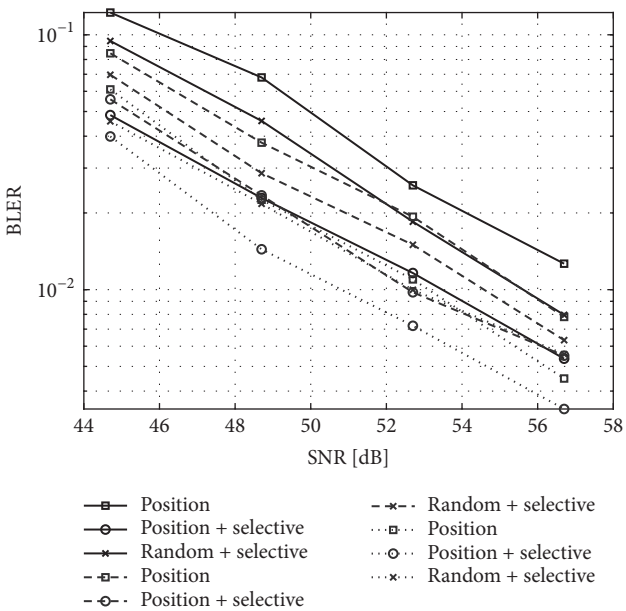

Figure 21: *BLER* versus *SNR* for *PDP* = 0.5 and different strategies, rate 1/3 for 5G LDPC, with different λ, 256-QAM modulation and $N = 1056$. Curves with solid lines are for $\lambda = 0.25$, curves with dashed lines are for $\lambda = 0.5$, and curves with doted lines are for $\lambda = 1.00$.

applied to multi-carrier transmission. The motivation behind this study is to find the most effective allocation strategies for managing the presence of subcarriers with different levels of signal-to-noise ratio, which are known apriori according to the half and full duplex patterns of the subcarriers or groups of subcarriers. We have investigated several encoding schemes, mainly derived from 3GPP specifications and adapted to the partial duplex system, and we have integrated them with allocation strategies of the encoded symbols in the subcarriers. According to the simulation results, the performance of positioning strategy with respect to random distribution generally shows better performance for LDPC codes while a random, simple distribution is the appropriate choice for the turbo codes. On the other hand, results show that 5G 3GPP LDPC is the best design choice for partial duplex, with respect to turbo and polar codes.

Data Availability

The data used to support the findings of this study are available from the corresponding author upon request.

Conflicts of Interest

The authors declare that there are no conflicts of interest regarding the publication of this paper.

References

[1] H. R. Barzegar, L. Reggiani, and L. Dossi, "Extending the range of full-duplex radio with multi-carrier partial overlapping," in *Proceedings of the 2017 International Symposium on Wireless Communication Systems (ISWCS)*, IEEE, Bologna, Italy, August 2017.

[2] I. Randrianantenaina, H. Elsawy, H. Dahrouj, and M.-S. Alouini, "Interference management with partial uplink/downlink spectrum overlap," in *Proceedings of the 2016 IEEE International Conference on Communications, ICC 2016*, 2016.

[3] A. AlAmmouri, H. ElSawy, O. Amin, and M.-S. Alouini, "In-Band α-Duplex Scheme for Cellular Networks: A Stochastic Geometry Approach," *IEEE Transactions on Wireless Communications*, vol. 15, no. 10, pp. 6797–6812, 2016.

[4] A. AlAmmouri, H. ElSawy, and M.-S. Alouini, "Flexible Design for α-Duplex Communications in Multi-Tier Cellular Networks," *IEEE Transactions on Communications*, vol. 64, no. 8, pp. 3548–3562, 2016.

[5] C. Yao, K. Yang, L. Song, and Y. Li, "X-Duplex: Adapting of Full-Duplex and Half-Duplex," in *Proceedings of the IEEE INFOCOM 2015 - IEEE Conference on Computer Communications Workshops (INFOCOM WKSHPS)*, IEEE, Hong Kong, China, April 2015.

[6] E. Arikan, "Channel polarization: a method for constructing capacity-achieving codes for symmetric binary-input memoryless channels," *IEEE Transactions on Information Theory*, vol. 55, no. 7, pp. 3051–3073, 2009.

[7] H. R. Barzegar and L. Reggiani, "LDPC encoding for partial-duplex wireless communication," in *Proceedings of the 2017 IEEE 28th Annual International Symposium on Personal, Indoor, and Mobile Radio Communications (PIMRC)*, pp. 1–5, IEEE, Montreal, QC, Canada, October 2017.

[8] 3GPP, "NR; Multiplexing and channel coding," 3rd Generation Partnership Project (3GPP), Technical Specification (TS) 38.212, 01 2018.

[9] 3GPP, "Evolved Universal Terrestrial Radio Access (E-UTRA); Multiplexing and channel coding," 3rd Generation Partnership Project (3GPP), Technical Specification (TS) 36.212, 12 2009.

[10] B. Tahir, S. Schwarz, and M. Rupp, "BER comparison between Convolutional, Turbo, LDPC, and Polar codes," in *Proceedings of the 2017 24th International Conference on Telecommunications (ICT)*, pp. 1–7, IEEE, Limassol, Cyprus, May 2017.

[11] M. Sybis, K. Wesolowski, K. Jayasinghe, V. Venkatasubramanian, and V. Vukadinovic, "Channel Coding for Ultra-Reliable Low-Latency Communication in 5G Systems," in *Proceedings of the 2016 IEEE 84th Vehicular Technology Conference (VTC-Fall)*, pp. 1–5, IEEE, Montreal, QC, Canada, September 2016.

[12] O. Iscan, D. Lentner, and W. Xu, "A Comparison of Channel Coding Schemes for 5G Short Message Transmission," in *Proceedings of the 2016 IEEE Globecom Workshops (GC Wkshps)*, pp. 1–6, IEEE, Washington, DC, USA, December 2016.

[13] X. Wu, M. Jiang, C. Zhao, L. Ma, and Y. Wei, "Low-Rate PBRL-LDPC Codes for URLLC in 5G," *IEEE Wireless Communications Letters*, vol. 7, no. 5, pp. 800–803, 2018.

[14] H. Gamage, N. Rajatheva, and M. Latva-aho, "Channel coding for enhanced mobile broadband communication in 5G systems," in *Proceedings of the 2017 European Conference on Networks and Communications (EuCNC)*, pp. 1–6, IEEE, Oulu, Finland, June 2017.

[15] T. Richardson and S. Kudekar, "Design of Low-Density Parity Check Codes for 5G New Radio," *IEEE Communications Magazine*, vol. 56, no. 3, pp. 28–34, 2018.

[16] H. Kim, "Coding and modulation techniques for high spectral efficiency transmission in 5G and satcom," in *Proceedings of the 2015 23rd European Signal Processing Conference (EUSIPCO)*, pp. 2746–2750, IEEE, Nice, France, August 2015.

[17] L. Yuan, J. Pan, N. Yang, Z. Ding, and J. Yuan, "Successive Interference Cancellation for LDPC Coded Non-Orthogonal Multiple Access Systems," *IEEE Transactions on Vehicular Technology*, 2018.

[18] X. Wu, C. Zhao, X. You, and S. Li, "Robust diversity-combing receivers for LDPC coded FFH-SS with partial-band interference," *IEEE Communications Letters*, vol. 11, no. 7, pp. 613–615, 2007.

[19] T. Tian and C. R. Jones, "Construction of rate-compatible LDPC codes utilizing information shortening and parity puncturing," *EURASIP Journal on Wireless Communications and Networking*, vol. 2005, no. 5, p. 692121, 2005.

[20] X. Liu, X. Wu, and C. Zhao, "Shortening for irregular QC-LDPC codes," *IEEE Communications Letters*, vol. 13, no. 8, pp. 612–614, 2009.

[21] R. G. Gallager, "Low-density parity-check codes," *IRE Transactions on Information Theory*, vol. 8, no. 1, pp. 21–28, 1962.

[22] F. R. Kschischang, B. J. Frey, and H.-A. Loeliger, "Factor graphs and the sum-product algorithm," *IEEE Transactions on Information Theory*, vol. 47, no. 2, pp. 498–519, 2001.

[23] C. Berrou, A. Glavieux, and P. Thitimajshima, "Near Shannon limit error-correcting coding and decoding: turbo-codes. 1," in *Proceedings of the IEEE International Conference on Communications (ICC '93)*, vol. 2, pp. 1064–1070, IEEE, Geneva, Switzerland, May 1993.

[24] T. ETSI, *"136 212 v10. 0.0.(2011)," Multiplexing and channel coding (3GPP TS 36.212 Ver. 10.0. 0 Release 10)*, France.

[25] H. Vangala, E. Viterbo, and Y. Hong, "A comparative study of polar code constructions for the AWGN channel," 2015, https://arxiv.org/abs/1501.02473.

[26] D.-M. Shin, S.-C. Lim, and K. Yang, "Design of length-compatible polar codes based on the reduction of polarizing matrices," *IEEE Transactions on Communications*, vol. 61, no. 7, pp. 2593–2599, 2013.

[27] V. Bioglio, C. Condo, and I. Land, "Design of polar codes in 5G new radio," 2018, https://arxiv.org/abs/1804.04389.